Chronology and structural control of Late Cenozoic volcanism in the Loma Creston quadrangle, southern Jemez volcanic field, New Mexico

Richard M. Chamberlin and William C. McIntosh
2007, pp. 248-261. https://doi.org/10.56577/FFC-58.248

in:

Geology of the Jemez Region II, Kues, Barry S., Kelley, Shari A., Lueth, Virgil W.; [eds.], New Mexico Geological Society 58 th Annual Fall Field Conference Guidebook, 499 p. https://doi.org/10.56577/FFC-58

This page is intentionally left blank to maintain order of facing pages.

New Mexico Geological Society Guidebook, 58th Field Conference, Geology of the Jemez Mountains Region II, 2007, p. 248-261.

CHRONOLOGY AND STRUCTURAL CONTROL OF LATE CENOZOIC VOLCANISM IN THE LOMA CRESTON QUADRANGLE, SOUTHERN JEMEZ VOLCANIC FIELD, NEW MEXICO

RICHARD M. CHAMBERLIN AND WILLIAM C. McINTOSH
New Mexico Bureau of Geology and Mineral Resources, Socorro, NM 87801, richard@gis.nmt.edu

Abstract — Geologic mapping and 29 new $^{40}Ar/^{39}Ar$ age determinations of seven major volcanic units confirm several episodes of mafic and silicic volcanism in the southern Jemez field in late Cenozoic time. Volcanism began with eruption of the aphyric basalt of Chamisa Mesa at approximately 9.9± 0.9 Ma. Overlying lava domes of the Canovas Canyon Rhyolite yield ages of 9.7 to 9.4 Ma. A second mafic pulse, the basalt of Bodega Butte (new name) is precisely dated at 9.14± 0.12 Ma (n= 4). A separate mapping project shows this 9.1 Ma olivine-augite basalt fills SW-descending paleovalleys near the base of a composite volcano of the Paliza Canyon Formation centered on Ruiz Peak, 10 km north of Loma Creston. We interpret the basalt of Bodega Butte as a late-stage flank eruption from the 9.5 to-9.1 Ma volcano at Ruiz Peak. Biotite from a Paliza Canyon trachydacite lava flow at Loma Creston is dated at 9.44± 0.16 Ma. The basalt of Bodega Butte apparently flowed southward around the low hill of dacite at Loma Creston. The trachyandesite of Mesita Cocida (new name), dated at 7.09± 0.21 Ma (n=3), is a microporphyritic, plagioclase-hornblende flow that unconformably overlies tilted volcaniclastic sediments at Mesita Cocida. Plinian pulses of the Bearhead Rhyolite at 7.0, 6.8 and 6.3 Ma produced the overlying Peralta Tuff and thin coeval ash beds. The final eruption in the study area was a xenocrystic basaltic andesite from a fissure vent on northwest Santa Ana Mesa at 2.4 Ma. Two episodes of hydrothermal alteration (ca. 9-8 and 7-5.3 Ma) are linked to crustal intrusions that fed ENE-trending vent zones of the Canovas Canyon and Bearhead rhyolites. Adularia from the red jasperoidal zone at Mesita Cocida is precisely dated at 5.31± 0.08 Ma. An en echelon belt of jasperized dextral-oblique normal faults at Mesita Cocida is aligned with a narrow transverse graben near Bodega Butte. The ENE-trending Bodega-Cocida shear zone (BCSZ) is interpreted as a preexisting basement structure, locally reactivated as a zone of distributed sinistral shear within the Rio Grande rift. We suggest that the BCSZ formed as the relatively "rigid" ENE-trending margin of the Colorado Plateau was dragged obliquely westward away from mobile lithosphere under the rift to create a focus of dilatant sinistral shear, which in turn controlled the ascent of late Miocene rhyolite intrusions under the southern Jemez volcanic field.

INTRODUCTION

The Loma Creston quadrangle (Chamberlin et al., 1999) spans the southern margin of the late Cenozoic Jemez volcanic field (Smith et.al, 1970) and the north margin of the Albuquerque Basin, a major north-trending axial basin of the northern Rio Grande rift (Chapin and Cather, 1994; Connell, 2004). At a regional scale, the Jemez volcanic field overlaps the tectonic boundary between relatively "rigid" lithosphere of the westward drifting Colorado Plateau (all motions are relative) and the mobile–westward stretching–lithosphere under the rift (Chapin and Cather, 1994). At the latitude of the Jemez field, axial basins of the northern rift form a right-stepping array where they obliquely cross a preexisting structural grain in basement rocks that is roughly coincident with a young volcanic zone known as the Jemez lineament (Chamberlin, 2007). The Jemez lineament is usually defined on maps as a broad ENE-trending linear zone of late Cenozoic basaltic volcanic fields that extend from Springerville, Arizona to Clayton, New Mexico. Popular explanations of the Jemez lineament is that it represents a "leaky crustal flaw" (Aldrich, 1986) or a fertile (easily melted) zone at the base of the lithospheric mantle, which is approximately coincident with the southern edge of the 1.7 to 1.65 Ga Yavapai-Mazatzal suture zone (Karlstrom and Humphreys, 1998). Our objectives are to present temporal, compositional and structural data pertinent to the late Miocene magmatic and tectonic evolution of the Colorado Plateau-Rio Grande rift boundary zone in the southern Jemez volcanic field.

Previous work

All geologic investigations of the Jemez volcanic field generally build on a solid foundation provided by the classic geologic map of the Jemez Mountains made by Smith et al. (1970). The wide coverage (6500 km^2) and obvious attention to volcanic features on this map is impressive when one remaps fragments (140 km^2) of the same terrane at a finer scale. Recent mapping to the south (Connell et al., 1995; Connell, 2006) has shown that formations of the lower and middle Santa Fe Group extend into the southern Loma Creston quadrangle where they intertongue with late Miocene volcanic strata of the southern Jemez field. Map relationships suggest that fluvial volcanic-rich conglomerates of the Navajo Draw Member of the Arroyo Ojito Formation (Connell et al., 1995; Connell, 2006) intertongue to the north with a syneruptive proximal facies of volcaniclastic rocks designated as the "Paliza Canyon Formation volcaniclastic sediments" (Lavine et al., 1996; p. 212).

Our perspective of volcanic stratigraphy and chronology in the southwestern Jemez Mountains differs somewhat from that of Gardner and Goff (1984) and Gardner et al. (1986). Most of these differences can be attributed to the inherently greater precision of the $^{40}Ar/^{39}Ar$ dating method compared to K-Ar dating. We suggest that distinctive mafic lava flow units should be, or remain, informally named where their physical stratigraphy is well established and their age is precisely constrained. Field observations (Chamberlin et al., 1999), age data (Table 1; Fig.1), geochemical

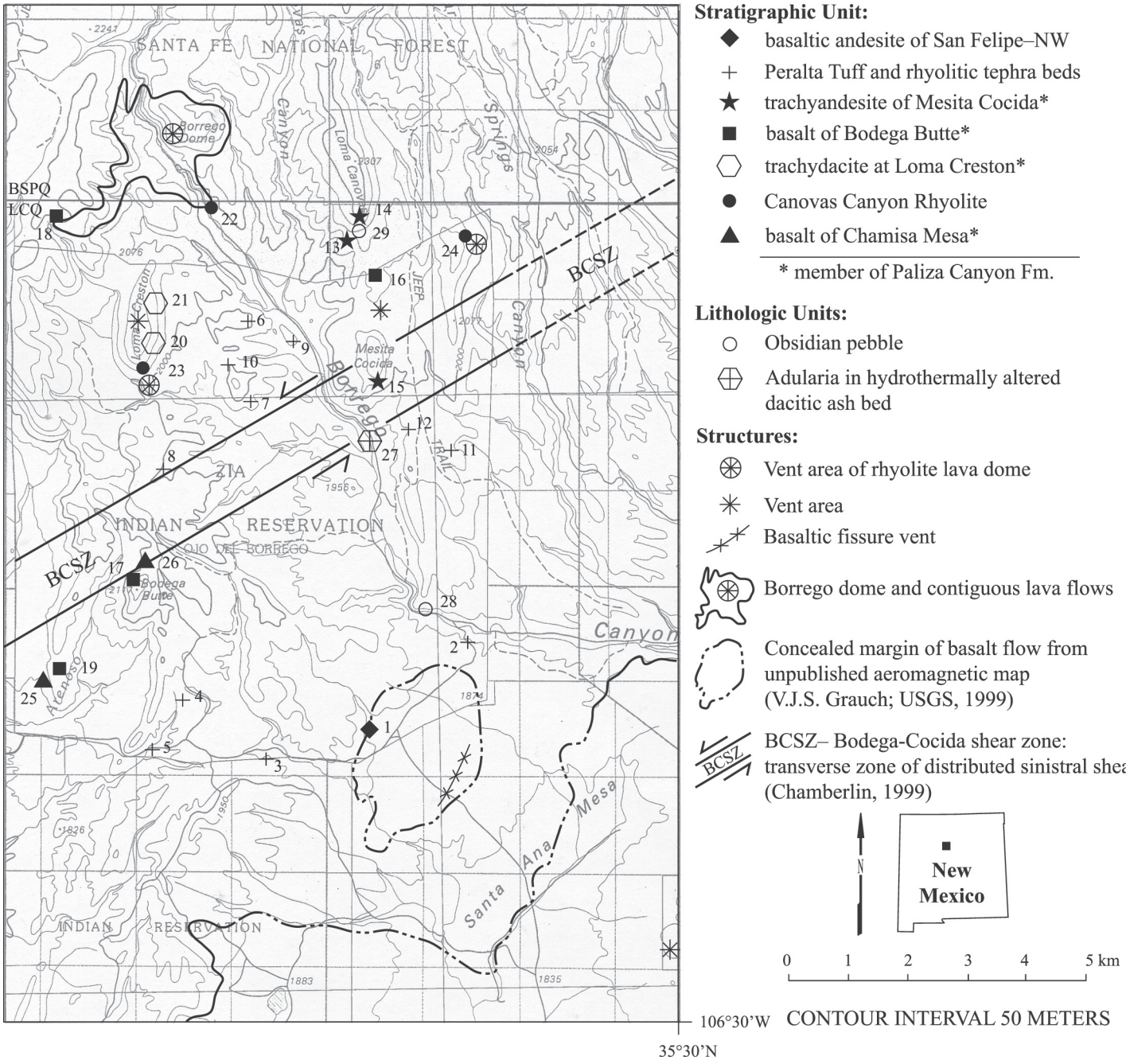

FIGURE 1. Location of $^{40}Ar/^{39}Ar$ dating samples and volcanic structures in the Loma Creston quadrangle (LCQ). Map numbers are keyed to Table 1. Structural data are from Chamberlin et al. (1999). Borrego Dome in Bear Springs Peak quadrangle (BSPQ) is from Smith et al. (1970).

data (Table 2; Fig. 2), and petrographic data (Table 3) summarized here generally support the physical volcanic stratigraphy of the lower portion of the Keres Group as outlined by Bailey et al. (1969) and mapped by Smith et al. (1970). Importantly, we now also recognize an erosional to angular unconformity within the upper Keres Group, that occurs at the base of volcanic strata younger than the 7.1 Ma trachyandesite of Mesita Cocida (new name) and the base of the more widespread Peralta Tuff dated at 6.9 Ma (McIntosh and Quade, 1995). This unconformity may be laterally equivalent to a widespread unconformity that separates middle and upper Santa Fe Group strata in the northwestern Albuquerque Basin (S. D. Connell, personal commun., 2006).

$^{40}Ar/^{39}Ar$ methods and results

Wherever possible the dense crystalline cores of mafic lava flows were preferentially sampled for $^{40}Ar/^{39}Ar$ dating. However, the finely vesicular (diktytaxitic) texture of the trachyandesite of Mesita Cocida made this approach impossible for that unit. Except for samples 4 and 7 (Table 1), all samples of pumiceous

TABLE 1. Summary of $^{40}Ar/^{39}Ar$ age determinations for the Loma Creston quadrangle; preferred and mean ages of eruption are listed in Table 4.

No.	Field No.	Unit	Lab No.	Material Dated	Method	n	Age (Ma)	± 2 σ	MSWD	K/Ca	± 2 σ	UTM-E	UTM-N
basaltic andesite of San Felipe--NW													
1	LC-98-9	Tbn	50139-01	groundmass	RHIF	6	2.46	0.22	2.3	0.15	nc	0358858	3934281
pumice bed from Cerrito Yelo													
2	LC-98-43	Tcyt	50253-01	sanidine	SCLF	13	6.29	0.08	0.41	79.3	10.5	0360520	3935838
sedimentary and fall deposits of the Peralta Tuff Member of the Bearhead Rhyolite													
3	GSZ-404B	Tbps	8938	sanidine	SCLF	13	6.79	0.09	0.56	43.6	11	0357080	3933948
4	5.18.98	Tbps	9747	sanidine	SCLF	12	6.80	0.02	2.7*	44.9	4.0	0355710	3934880
5	LC-98-36	Tbps	50248	sanidine	SCLF	9	6.81	0.08	0.48	47.2	7.2	0355153	3934080
6	LC-99-11	Tbps	50510	sanidine	SCLF	17	6.90	0.06	0.28	42.3	10.5	0356920	3941240
7	GSZ-429C	Tbps	9744	sanidine	SCLF	14	6.92	0.02	4.8*	47.8	10.2	0356900	3939920
8	LC-99-4	Tbps	50507	sanidine	SCLF	12	6.93	0.06	0.43	40.0	3.4	0355398	3938778
9	LC-99-10	Tbps	50509	sanidine	SCLF	4	7.02	0.12	0.16	46.1	4.4	0357704	3940920
10	LC-99-9	Tbps	50508	plagioclase	SCLF	15	7.03	0.54	0.36	0.62	0.09	0356583	3940499
Peralta Tuff Member of the Bearhead Rhyolite													
11	LC-99-5A	Tbp	50250	sanidine	SCLF	14	6.89	0.14	0.23	51.7	10.9	0360300	3939077
12	LC-98-25B	Tbp	50251	sanidine	SCLF	12	6.73	0.38	1.6	47.2	7.2	0359621	3939441
trachyandesite of Mesita Cocida, upper member of the Paliza Canyon Formation													
13	LC-98-13	Tpmc	50140-01	groundmass	RHIF	6	6.79	0.24	2.5	0.15	nc	0358668	3942739
14	LC-98-31	Tpmc	50238-01	groundmass	RHIF	5	7.16	0.13	4.0*	0.37	nc	0358858	3943057
15	GSZ-431C	Tpmc	9738-01	groundmass	RHIF	8	7.18	0.26	0.5	0.62	nc	0359100	3940205
basalt of Bodega Butte, medial member of the Paliza Canyon Formation													
16	GSZ-493	Tpbb	9739-02	groundmass	RHIF	8	9.04	0.18	1.0	0.51	nc	0359060	3942065
17	LC-98-4	Tpbb	50104-01	groundmass	RHIF	6	9.04	0.12	1.7	0.3	nc	0355009	3936878
18	LC-98-5	Tpbb	50105-01	groundmass	RHIF	9	9.17	0.10	2.0	0.24	nc	0353720	3943031
19	LC-98-2	Tpbb	50101-01	groundmass	RHIF	7	9.25	0.13	3.7*	0.28	nc	0353860	3935403
trachydacite at Loma Creston, lower member of the Paliza Canyon Formation													
20	6.13.98.1	Tpd	9745-01	hornblende	RHIF	10	9.23	0.96	0.6	0.86	nc	0355025	3940880
21	LC-99-2	Tpd	50260-01	biotite	RHIF	10	9.44	0.16	0.55	13.1	nc	0355104	3941442
Canovas Canyon Rhyolite and tephra facies													
22	LC-98-14	Tcc	50252-01	biotite	RHIF	4	9.54	0.14	2.5	35.9	nc	0356303	3943278
23	LC-98-8	Tcc	50103-01	whole rock	RHIF	6	9.72	0.14	4.6*	7.5	nc	0355199	3940517
24	LC-98-23	Tcct	50254-01	biotite	RHIF	isochron	9.74	0.23	15*	18.1	nc	0360635	3942680
basalt of Chamisa Mesa, basal member of the Paliza Canyon Formation													
25	LC-98-1	Tpcm	50100-01	groundmass	RHIF	isochron	9.02	0.76	0.47	0.16	nc	0353397	3935202
26	LC-98-3	Tpcm	50102-01	groundmass	RHIF	isochron	10.77	1.8	0.43	0.12	nc	0355090	3937112
Age of hydrothermal alteration (jasperoid and potassic alteration)													
27	LC-98-11	Tpvs	50121	adularia	SCLF	11	5.31	0.08	1.4	192.8	244.4	0358955	3939302
Maximum age of volcaniclastic sedimentary units													
28	LC-98-28	Tc	50237-01	obsidian	RHIF	12	6.35	0.20	1.90	8.2	nc	0359775	3936380
29	LC-98-32	Tpvs	50236-01	odsidian	RHIF	7	9.38	0.06	1.7	10.6	nc	0358823	3942811

NOTES: Method is single crystal laser fusion (SCLF) or resistance furnace incremental heating (RFIH). Except for isochron ages, n is number of individual crystal analyzed (SCLF) or number of heating steps used to calculate weighted mean age (RFIH) , K/Ca is molar ratio calculated from K-derived 39Ar and Ca-derived 37Ar. Two-sigma variance not calculated (nc) for RHIF samples. Mean sum weighted deviates (MSWD) value with asterisk(*) indicates confidence interval less than 95%.

Methods: Sample preparation: sanidine, plagioclase, biotite –crushing, LST heavy liquid, Franz, HF; groundmass concentrate – crushing, picking. Irradiation: four separate in vacuo 7-14 hr irradiations (NM-50, NM-69, NM-75, NM-77), D-3 position, Nuclear Science Center, College Station, TX. Neutron flux monitor Fish Canyon Tuff sanidine (FC-2). Assigned age = 28.02 Ma (Renne et al., 1998); samples and monitors irradiated in alternating holes in machined Al disks.

Laboratory: New Mexico Geochronology Research Laboratory, Socorro NM. Instrumentation: Mass Analyzer Products 215-50 mass spectrometer on line with automated all-metal extraction system. Heating: sanidine – SCLF, 10W continuous CO2 laser; RFIH – 25 –45 mg aliquots in resistance furnace. Reactive gas cleanup: SAES GP-50 getters operated at 20°C and ~450 °C; SCLF – 1 to 2 minutes, RFIH – 9 minutes. Error calculation: all errors reported at ±2 sigma, mean ages calculated using inverse variance weighting of Samson and Alexander (1987); decay constant and isotopic abundances: Steiger and Jaeger (1977).

Analytical parameters: electron multiplier sensitivity = 1 to 3 x 10-17 moles/pA; typical system blanks were 470, 3 , 0.6 , 3, 3.0 x 10-18 moles (laser) and at 470, 3 , 0.6 , 3, 3.0 (furnace) at masses 40, 39, 38, 37, 36 respectively; J-factors determined to a precision of ± 0.2% using SCLF of 4 to 6 crystals from each of 4 to 6 radial positions around irradiation vessel. Correction factors for interfer nuclear reactions, determined using K-glass and CaF2, (40Ar/39Ar) K = 0.00020±0.0003; (36Ar/37Ar) Ca = 0.00026±0.00002; and (39Ar/37Ar) Ca = 0.00070±0.00005.

Samples: Samples are listed in observed or inferred stratigraphic order. Collected by Richard Chamberlin (LC), Gary Smith (GSZ), and Karl Wegmann (date of sampling). UTM sample locations are based on 1927 NAD. Map unit names are listed in Table 4.

rhyolite tephra were scraped clean of adhered sand grains at the time of collection. In most cases, two or more samples were collected from separate outcrop belts of the same unit in order to test field correlations based on physical stratigraphy. Where physical correlation was uncertain, some hydrothermally altered samples were collected if they contained fresh clear sanidine or black shiny biotite. These minerals tend to resist recrystallization in zones of potassic alteration (Chamberlin et al., 2004).

Results of 29 age determinations using the $^{40}Ar/^{39}Ar$ method are listed in Table 1. All samples were prepared and analyzed at the New Mexico Geochronology Research Laboratory at New Mexico Tech in Socorro. Fish Canyon Tuff sanidine, with an assumed age of 28.02 Ma, was used as a monitor for reducing the analytical data (Renne et al., 1998). Complete analytical data,

including age spectrum diagrams, for the Loma Creston quadrangle are available on line (McIntosh et al., 2007).

Geochemistry methods and results

Where possible, two or more representative samples of volcanic units were collected from different outcrop belts for XRF geochemical analysis at the New Mexico Bureau of Geology (Table 2). Chemical data generally support the initial field correlations and supplement the correlations based on age data (Table 1). In some cases hydrothermally silicified rocks were collected on purpose, to allow comparison of immobile element ratios (e.g., Nb/Y and Zr/TiO2) as a means of correlation to possible unaltered equivalents. Figure 2 shows the chemical classification of unaltered samples from Table 2; hydrated and leached samples of Peralta Tuff are the only exception. Most of these unaltered rock samples are only slightly alkaline. One sample of relatively alkaline trachyandesite porphyry (Fig. 2; Table 2, I) could alternatively be classified as a benmoreite porphyry, especially if it were in an oceanic island setting. Samples of the Peralta Tuff are hydrated (LOI > 10%) and sodium is anomalously low for a rhyolite; leaching of sodium from hydrated siliceous glasses is common and well known.

Petrographic data

General petrographic descriptions of representative thin sections from the major lava units are summarized in Table 3. Petrographic names of the lavas are primarily based on phenocryst mineralogy and textural analysis, which is then used as a modifier to the geochemical classification. Mineral names in front of chemical classes list the phenocrystic phases present, in order of decreasing abundance. Microphenocrysts, which can be difficult to see in hand specimen (usually slender or less than 0.5 mm long), are described as fine grained and the host rock is called microporphyritic. Large obvious phenocrysts (usually plagioclase), greater than 4 mm long, are described as coarse grained and the host rock is typically called a porphyry. Visually estimated total phenocryst content is described as sparse or phenocryst-poor, if less than 5%, and abundant or phenocryst-rich if more than 25%. The groundmass of basalts typically consists of plagioclase microlites plus interstitial pyroxene, olivine and opaque Fe-Ti oxides. The groundmass of dacites and rhyolites is typically cryptocrystalline or glassy. Colors reported here are those most commonly observed on dry, freshly broken surfaces of hand specimens from unaltered or unoxidized (non-reddened) outcrops.

CHRONOLOGY AND CORRELATION OF VOLCANIC UNITS

Figure 3 graphically illustrates age constraints and correlation of late Miocene volcanic units in the northern half of the Loma Creston quadrangle. Considering analytical error, the age data are in good agreement with the physical stratigraphic relationships as mapped by Chamberlin et al. (1999).

Relatively widespread and distinctive basaltic flow units provide the most useful reference horizons with respect to the correlation of relatively lenticular flows of intermediate to silicic composition and discontinuous rhyolitic tephra. Limited geochemical and petrographic data (Tables 2, 3) suggest that the late Miocene basaltic flow units (Table 4) are laterally zoned with respect to minor variations in phenocryst mineralogy and composition. Some flow units may represent coalesced flow lobes of similar composition and stratigraphic position. All mafic to intermediate flow units of late Miocene age described below are regarded as stratigraphically distinct members of the Paliza Canyon Formation (cf. Lavine et al., 1996).

Basalt of Chamisa Mesa

The basalt of Chamisa Mesa is the stratigraphically lowest lava flow exposed in the study area and apparently in the southwest Jemez volcanic field (Bailey et al., 1969; Smith et al. 1970; Chamberlin et al., 1999). It is typically a dark gray to black aphyric diabasic lava that locally grades laterally into fine-grained phenocryst-poor olivine basalt. Aphyric and ophitic textures (Table 3, X) imply that it erupted near its liquidus temperature. This flow unit is typically about 6-12 m thick and it generally thickens northward toward a presumed source vent area under Borrego Mesa. A terminus of the flow is locally exposed within sandstones of the Cerro Conejo Formation about 2 km south of Bodega Butte. The basalt of Chamisa Mesa is also absent near Bear Springs, about 8 km NE of Loma Creston (Smith et al., 1970).

Dense samples of the basalt of Chamisa Mesa from Arroyo Arenoso and the north flank of Bodega Butte produced relatively

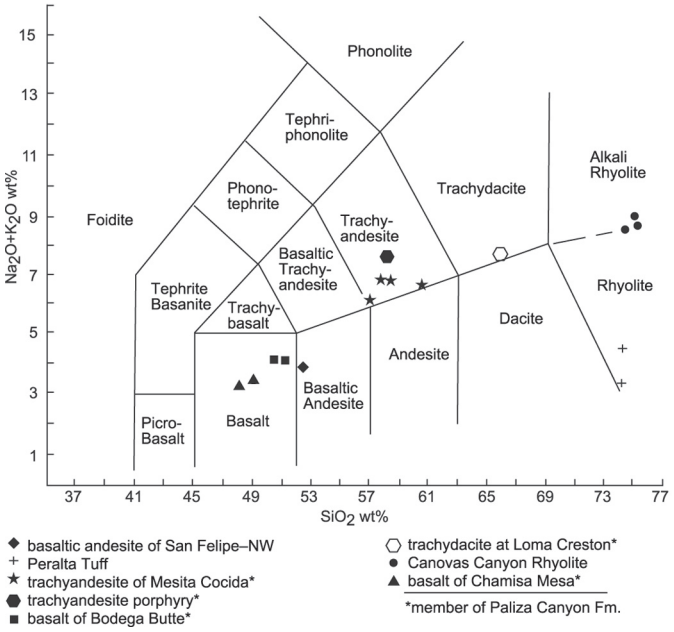

FIGURE 2. Chemical classification of volcanic rock samples from the Loma Creston quadrangle based on the IUGS total-alkali vs. silica scheme of Le Bas et al. (1986). Data are from Table 2; see text for discussion.

TABLE 2. Summary of whole-rock geochemical data for the Loma Creston quadrangle.

ID.	Field No.	Unit	SiO2	TiO2	Al2O3	Fe2O3-T	MnO	MgO	CaO	K2O	Na2O	P2O5	LOI	Total	n SiO2	n Alkali	UTM E	UTM N	Comment
basaltic andesite of San Felipe NW																			
A	**LC-98-9**	Tbn	52.58	1.36	15.76	10.87	0.15	6.22	9.02	0.65	3.25	0.22	-0.01	100.08	52.53	3.90	0358858	3934281	
Peralta Tuff Member of the Bearhead Rhyolite																			
B	*LC-98-34*	*Tbp*	*60.32*	*0.12*	*11.91*	*0.70*	*0.06*	*1.43*	*4.04*	*1.68*	*0.97*	*0.02*	*18.76*	*100.00*	*74.25*	*3.26*	*0359382*	*3940623*	*hydrated*
C	***LC-99-5A***	*Tbp*	*75.70*	*0.20*	*8.49*	*1.12*	*0.04*	*0.86*	*2.13*	*1.48*	*0.54*	*0.06*	*9.57*	*100.19*	*83.54*	*2.23*	*0360300*	*3939077*	*silicified*
D	**LC-98-25A**	Tbp	63.29	0.13	12.78	0.74	0.03	1.01	3.06	3.38	0.49	0.03	14.04	98.97	*74.52*	*4.56*	0359621	3939441	*hydrated*
trachyandesite of Mesita Cocida, upper member of Paliza Canyon Formation																			
E	**LC-98-13**	Tpmc	56.91	1.35	16.90	7.21	0.15	2.63	5.69	2.08	4.61	0.76	0.77	99.05	58.03	6.88	0358668	3942739	
F	**LC-98-31**	Tpmc	57.25	1.35	16.93	7.26	0.15	2.63	5.73	2.15	4.68	0.76	0.77	99.66	57.89	6.91	0358858	3943057	
G	LC-98-15	Tpmc	55.95	1.37	16.92	7.79	0.13	3.00	6.63	1.89	4.23	0.61	1.40	99.92	56.79	6.21	0358190	3941043	
H	LC-98-18	Tpmc	59.12	1.10	16.65	6.18	0.11	2.25	5.27	2.28	4.24	0.54	1.37	99.10	60.49	6.67	0359655	3943020	
trachyandesite porphyry member of the Paliza Canyon Formation																			
I	LC-98-12	Tpa	56.98	1.36	16.78	7.34	0.08	2.06	5.30	2.98	4.64	0.59	1.86	99.96	58.08	7.77	0360005	3943235	
basalt of Bodega Butte, medial member of the Paliza Canyon Formation																			
J	*LC-98-29*	*Tpbb*	*51.27*	*1.46*	*17.39*	*9.24*	*0.10*	*3.03*	*8.55*	*1.69*	*3.94*	*0.64*	*2.56*	*99.88*	*52.68*	*5.79*	*0359080*	*3942095*	*propylitized*
K	*LC-98-22*	*Tpbb*	*48.20*	*1.75*	*17.13*	*9.87*	*0.13*	*3.53*	*10.19*	*1.56*	*3.30*	*0.54*	*3.43*	*99.62*	*50.11*	*5.05*	*0360232*	*3943157*	*propylitized*
L	**LC-98-4**	Tpbb	49.80	1.53	15.00	10.91	0.16	7.20	9.69	0.85	3.25	0.43	0.98	99.80	50.40	4.15	0355009	3936878	
M	**LC-98-5**	Tpbb	50.86	1.53	15.49	10.89	0.16	7.03	9.28	0.84	3.32	0.39	0.02	99.80	50.97	4.17	0353720	3943031	
N	***LC-98-2***	*Tpbb*	*49.26*	*1.54*	*16.12*	*11.12*	*0.17*	*3.34*	*10.11*	*0.83*	*3.34*	*0.43*	*2.98*	*99.25*	*51.17*	*4.33*	*0353860*	*3935403*	*propylitized*
trachydacite flow at Loma Creston, lower member of the Paliza Canyon Formation																			
O	**LC-99-2**	Tpd	64.54	0.71	16.69	3.82	0.08	1.18	3.39	2.95	4.64	0.24	1.30	99.55	65.69	7.73	0355104	3941442	
Canovas Canyon Rhyolite and tephra facies																			
P	*LC-98-16*	*Tcc*	*81.86*	*0.08*	*9.57*	*0.50*	*0.02*	*0.02*	*0.17*	*5.71*	*1.61*	*0.02*	*0.65*	*100.20*	*82.23*	*7.35*	*0360680*	*3942382*	*silicified*
Q	LC-98-6	Tcc	74.71	0.19	13.71	1.08	0.06	0.12	0.73	4.49	4.48	0.04	0.28	99.89	75.00	9.01	0353902	3942838	
R	**LC-98-14**	Tcc	72.37	0.22	13.76	1.18	0.06	0.31	0.94	4.40	4.01	0.04	2.90	100.19	74.38	8.64	0356303	3943278	
S	**LC-98-8**	Tcc	74.20	0.17	13.48	0.94	0.06	0.13	0.94	4.50	4.35	0.05	0.88	99.70	75.09	8.96	0355199	3940517	
T	*LC-99-1*	*Tcct*	*45.55*	*0.28*	*9.86*	*1.41*	*0.05*	*0.90*	*17.88*	*3.36*	*1.64*	*0.08*	*19.08*	*100.09*	*56.23*	*6.17*	*0356281*	*3938659*	*calcite*
U	*LC-98-24*	*Tcct*	*70.84*	*0.12*	*11.51*	*0.83*	*0.04*	*0.55*	*2.05*	*3.92*	*1.32*	*0.02*	*9.10*	*100.30*	*77.68*	*5.75*	*0360380*	*3942800*	*silicified*
V	*LC-98-17*	*Tcct*	*71.96*	*0.11*	*10.41*	*0.62*	*0.03*	*0.27*	*1.46*	*4.83*	*1.04*	*0.02*	*8.73*	*99.48*	*79.30*	*6.47*	*0360602*	*3942525*	*silicified*
W	***LC-98-23***	*Tcct*	*77.89*	*0.13*	*11.97*	*0.57*	*0.02*	*0.05*	*0.32*	*6.16*	*2.63*	*0.02*	*0.60*	*100.36*	*78.08*	*8.81*	*0360635*	*3942680*	*silicified*
basalt of Chamisa Mesa, basal member of the Plaiza Canyon Formation																			
X	**LC-98-1**	Tpcm	46.69	1.51	15.39	10.70	0.17	5.53	11.82	0.47	2.86	0.31	5.09	100.54	48.91	3.49	0353397	3935202	
Y	**LC-98-3**	Tpcm	46.64	1.56	16.33	11.12	0.16	7.37	10.52	0.41	2.80	0.30	3.06	100.27	47.97	3.30	0355090	3937112	

Trace element data

ID.	Field No.	Unit	Sr	Rb	Th	Pb	Ga	Zn	Cu	Ni	Cr	Ba	V	As	U	Y	Zr	Nb	Mo
basaltic andesite of San Felipe NW																			
A	**LC-98-9**	Tbn	392	16	ND	2	18	91	60	75	178	350	175	3	2	25	136	7	ND
Peralta Tuff Member of the Bearhead Rhyolite																			
B	*LC-98-34*	*Tbp*	*692*	*57*	*9*	*19*	*10*	*27*	*4*	*3*	*ND*	*507*	*8*	*3*	*3*	*8*	*92*	*17*	*ND*
C	***LC-99-5A***	*Tbp*	*1253*	*32*	*5*	*13*	*10*	*26*	*7*	*8*	*11*	*881*	*22*	*6*	*4*	*17*	*103*	*9*	*ND*
D	**LC-98-25A**	Tbp	2002	435	14	12	17	33	6	4	5	437	10	41	3	14	94	14	ND
trachyandesite of Mesita Cocida, upper member of Paliza Canyon Formation																			
E	**LC-98-13**	Ttmc	752	38	3	13	20	91	5	3	ND	1102	73	3	3	44	262	20	ND
F	**LC-98-31**	Ttmc	745	37	5	12	20	90	5	4	4	1103	87	4	4	42	258	20	ND
G	LC-98-15	Ttmc	867	33	4	12	20	85	7	3	ND	1065	119	4	4	34	210	16	ND
H	LC-98-18	Ttmc	772	41	6	14	19	69	12	6	9	1284	85	4	4	29	220	17	ND
trachyandesite porphyry member of the Paliza Canyon Formation																			
I	LC-98-12	Tpa	894	62	8	17	20	85	21	16	14	1351	107	11	4	33	308	30	2
basalt of Bodega Butte, medial member of the Paliza Canyon Formation																			
J	*LC-98-29*	*Tpbb*	*1358*	*29*	*9*	*13*	*21*	*85*	*37*	*76*	*111*	*1193*	*229*	*111*	*5*	*27*	*210*	*23*	*ND*
K	*LC-98-22*	*Tpbb*	*1155*	*36*	*3*	*7*	*21*	*84*	*49*	*32*	*36*	*1017*	*216*	*16*	*2*	*35*	*170*	*19*	*ND*
L	**LC-98-4**	Tpbb	898	10	ND	7	18	91	72	130	309	764	197	5	2	27	141	10	ND
M	**LC-98-5**	Tpbb	826	14	ND	7	19	92	72	108	262	772	194	4	3	27	139	9	ND
N	***LC-98-2***	*Tpbb*	*921*	*11*	*ND*	*6*	*19*	*101*	*61*	*127*	*316*	*869*	*262*	*146*	*3*	*27*	*141*	*10*	*ND*
trachydacite flow at Loma Creston, lower member of the Paliza Canyon Formation																			
O	**LC-99-2**	Tpd	704	43	10	20	19	57	9	6	6	1180	55	4	6	24	210	27	1
Canovas Canyon Rhyolite and tephra facies																			
P	*LC-98-16*	*Tcc*	*28*	*183*	*14*	*25*	*11*	*13*	*ND*	*2*	*ND*	*212*	*7*	*4*	*6*	*12*	*64*	*34*	*ND*
Q	LC-98-6	Tcc	126	102	17	23	15	27	5	4	ND	901	5	3	8	21	147	34	ND
R	**LC-98-14**	Tcc	168	93	13	23	15	33	4	3	5	962	10	2	7	19	167	32	3
S	**LC-98-8**	Tcc	107	94	16	27	15	28	6	7	ND	942	11	2	7	20	136	35	ND
T	*LC-99-1*	*Tcct*	*317*	*60*	*6*	*12*	*11*	*32*	*4*	*4*	*6*	*717*	*15*	*3*	*5*	*13*	*137*	*20*	*1*
U	*LC-98-24*	*Tcct*	*431*	*179*	*15*	*28*	*14*	*26*	*5*	*3*	*ND*	*544*	*7*	*5*	*7*	*16*	*82*	*35*	*ND*
V	*LC-98-17*	*Tcct*	*1016*	*294*	*13*	*21*	*13*	*24*	*6*	*3*	*6*	*669*	*8*	*17*	*6*	*16*	*89*	*27*	*ND*
W	*LC-98-23*	*Tcct*	*58*	*179*	*12*	*25*	*15*	*10*	*3*	*3*	*4*	*727*	*8*	*8*	*6*	*13*	*85*	*30*	*ND*
basalt of Chamisa Mesa, basal member of the Plaiza Canyon Formation																			
X	**LC-98-1**	Tcb	572	10	ND	1	18	76	52	87	199	288	184	15	2	23	107	7	ND
Y	**LC-98-3**	Tcb	510	8	ND	ND	18	79	70	76	180	319	212	2	3	28	128	7	ND

NOTES: Oxides are in weight percent; elements are in ppm; na = not analysed; ND= not detected; LOI= loss on ignition Fe2O3-T is total iron expressed as Fe2O3. "nSiO2" is SiO2 normalized to 100% and volatile free. "n Alkali" is total alkalis normalized to 100% and volatile free. Normalized data of unaltered and propylitized samples are plotted on Figure 2.

Analytical Methods: Wavelength dispersive XRF spectrometry was used for major and trace element analyses.Major elements were analyzed with fused glass disks. Fused disks were prepared following the basic methods described by Norris and Hutton (1969). Approximately 1 g of sample was fused with 6 g of Sigma 12:22 flux, 50 mg of LiNO3, and 50 mg LiBr. Trace elements were determined on whole rock pressed powder pellets following Norrish and Chappell (1977). Seven grams of powdered sample were mixed with 7 drops of a 1% polyvinyl alcohol solution and pressed at ten tons with a boric acid backing. Analyses by Chris McKee at the New Mexico Tech XRF lab. The XRF lab at NMT was partly funded by NSF grant EAR93-16467. .

Samples: Sample numbers shown in bold font have been dated by Ar-Ar method (Table1). Data in italics represent hydrothermally altered rocks. Listed in approximate stratigraphic order. UTM sample locations are based on 1927 NAD

TABLE 3. Petrographic descriptions of lava flow units in the Loma Creston quadrangle.

ID.	Unit	Field No.	Petrographic description
basaltic andesite of San Felipe NW			
A	Tbn	**LC-98-9**	Dark gray, sparsely porphyritic olivine (2%),plagioclase (fine gr., 10%) basaltic andesite with rare xenocryst of quartz
trachyandesite of Mesita Cocida, upper member of Paliza Canyon Formation			
F	Tpmc	**LC-98-31**	Dark gray to black, micro-vesicular, aphyric looking (microporphyritic), plagioclase-rich (fine gr., 30%), hornblende (3%, oxidized) trachyandesite, with 15% ragged fine vesicles (diktytaxitic). Rare, fine iddingsite suggests basaltic component.
G	Tpmc	LC-98-15	Very similar to LC-98-31, 20% fine ragged vesicles, some vesicles have glassy walls. Trace of fine iddingsdite
H	Tpmc	LC-98-18	Similar to LC-98-31, more dense, only slightly vesicular (5%) with some unoxidixed hornblende. Lacks fine iddingsite observed at other localities.
trachyandesite porphyry member of the Paliza Canyon Formation			
I	Tpa	LC-98-12	Medium gray, phenocryst-rich, plagioclase (30%)-clinopyroxene (4%)-biotite (<1%) andesite porphyry with small glomerophyric fragments of plagioclase-pyroxene diorite
basalt of Bodega Butte, medial member of the Paliza Canyon Formation			
J	Tpbb	LC-98-29	Medium gray, moderately porphyritic "olivine" (4 %)-augite (2%)-plagioclase (1%) basalt. Propylitically altered; olivine altered to iddingsite+ chlorite+ quartz
L	Tpbb	**LC-98-4**	Medium to dark gray, sparsely porphyritic, olivine (4%, med. gr.) basalt with traces of phyric plagioclase, uniform rims (~0.2mm) of iddingsite on olivine suggest pre-eruption hydration in magma chamber.
M	Tpbb	**LC-98-5**	Medium to dark gray, sparsely porphyritic olivine (3 %, med gr.) basalt with traces of phyric clinopyroxene, olivine has very narrow rims of iddingsite that are chatoyant in hand specimen
trachydacite flow at Loma Creston, lower member of the Paliza Canyon Formation			
O	Tpd	**LC-99-2**	Medium gray, sparsely porphyritic hornblende (3% fine- to medium-grained, seriate with oxidized rims)-plagioclase (1%) trachydacite with aligned crystals (trachytic).
Canovas Canyon Rhyolite			
R	Tcc	**LC-98-14**	Light to medium gray, flow banded, slightly spherulitic, very phenocryst-poor, plagioclase (1%) -biotite (<0.5%) rhyolite
basalt of Chamisa Mesa, basal member of the Paliza Canyon Formation			
X	Tpcm	**LC-98-1**	Black, aphyric diabasic basalt with ophitic clinopyroxene, ophitic olivine (altered) and ophitic carbonate of uncertain origin. Trace of phyric iddingsite
Y	Tpcm	**LC-98-3**	Dark gray, very phenocryst poor, "olivine" (2% fine iddingsite) basalt with subophitic clinopyroxene

Notes: See Table 2 for sample location data, linked by ID letter. Field number shown in bold font indicates sample dated by $^{40}Ar/^{39}Ar$ method (Table 1).

imprecise isochron ages of 9.02± 0.76 and 10.77± 1.8 Ma (Table 1, no. 25, 26; Fig.3A). These dates are consistent with stratigraphy, in that they overlap with the age of the more precisely dated and stratigraphically higher basalt of Bodega Butte (Fig. 3). Averaging these two results yields a mean age of 9.9± 0.9 Ma for the basalt of Chamisa Mesa, which is compatible with all stratigraphic constraints from dated units in the quadrangle (Fig. 3; Table 1). Luedke and Smith (1978), published a whole-rock K-Ar age of 10.4± 0.5 Ma, analytically equivalent to our preferred mean age. The lowest basaltic flow unit on Borrego Mesa, 8 km NNW of Loma Creston, appears to be correlative with the basalt of Chamisa Mesa (S. Kelley, personal commun., 2007). At Borrego Mesa, this nearly aphyric basalt has yielded $^{40}Ar/^{39}Ar$ ages of 9.44± 0.45 and 9.37± 0.28 Ma (Osburn et al., 2002), which are also analytically acceptable with respect to age data for the overlying Canovas Canyon Rhyolite lavas (Fig. 3A). Gardner et al. (1986), recommended abandoning the basalt of Chamisa Mesa as a stratigraphic unit because of chemical similarities to Paliza Canyon Formation basaltic rocks. However, in the Loma Creston quadrangle it appears to be a distinctive mappable unit consistent with the map data of Smith et al. (1970). We recommend that the basalt of Chamisa Mesa of Smith et al. (1970), be reinstated as an informal flow unit. We reassign it as the basal member of the Paliza Canyon Formation in the southwestern Jemez Mountains.

Canovas Canyon Rhyolite

Canovas Canyon Rhyolite typically consists of light gray, phenocryst-poor, rhyolite lava domes, peripheral lava flows (Figs.1, 2, 3A; Table 3) and cogenetic tephras (Fig. 3A) that overlie the basalt of Chamisa Mesa in the northwest quadrant of the study area. Flows and domes form “stubby” exposures generally greater than 40 to 80 m in thickness. They are usually flow banded and locally display glassy toes that were presumably preserved under eolian sandstones of the Cerro Conejo Formation (Fig. 3A at Borrego Mesa). Sparse, small phenocrysts of plagioclase and traces of biotite are characteristic of Canovas Canyon lavas and tephras in the study area; sanidine phenocrysts are usually absent. Phenocryst-poor rhyolite ash beds that are stratigraphically equivalent to the Canovas Canyon lava domes lie only a few meters above

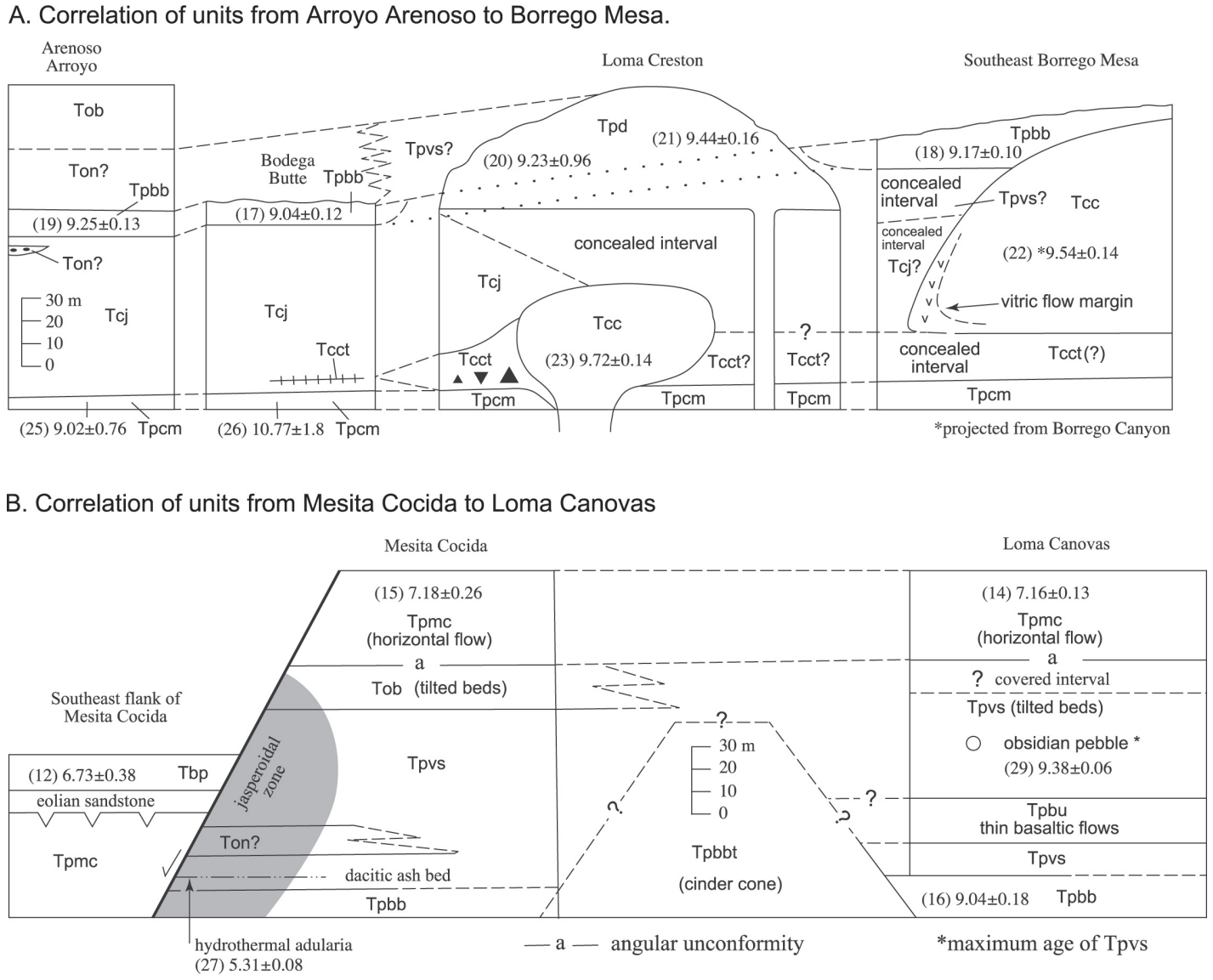

Units: Arroyo Arenoso to Borrego Mesa

Tob: Loma Barbon Member of the Arroyo Ojito Fm. of Connell, 1995
Tpvs: "Paliza Canyon Fm. volcaniclastic sediments"* of Lavine et al., 1996
Ton: Navajo Draw Member of the Arroyo Ojito Fm. of Connell, 1995
Tpd: trachydacite at Loma Creston*
Tpbb: basalt of Bodega Butte* (new name)
Tcj: Cerro Conejo Fm. of Connell, 1995
Tcc: Canovas Canyon Rhyolite
Tcct: Canovas Canyon Rhyolite tephra
Tpcm: basalt of Chamisa Mesa*

Units: Mesita Cocida to Loma Canovas

Tbp: Peralta Tuff
Tpmc: trachyandesite of Mesita Cocida* (new name)
Tob: Loma Barbon Member of the Arroyo Ojito Fm. of Connell, 1995
Tpvs: "Paliza Canyon Fm. volcaniclastic sediments"* of Lavine et al., 1996
Tpbu: unnamed basaltic flows*.
Tpbb: basalt of Bodega Butte* (new name)
Tpbbt: basalt of Bodega Butte, tephra facies*

* memeber of Paliza Canyon Fm.

FIGURE 3. Stratigraphic correlation diagrams based on geologic map data of Chamberlin et al. (1999), and $^{40}Ar/^{39}Ar$ age data summarized in Table 1. Thickness of each unit is estimated (± 20%) from structure sections and field observations. Concealed contacts are dashed. Ages are in millions of years (Ma); numbers in parentheses refer to map number on Figure 1 and in Table1. In A, black triangles in Tcct represent large basalt xenoliths in a proximal tuff breccia, and the dotted projection of Tpbb through Loma Creston (Tpd) indicates both units laterally occupy the same stratigraphic position. In B, shaded area under Mesita Cocida represents a tabular zone of red jasperoidal silica alteration (Fig.4). See text for discussion.

the basalt of Chamisa Mesa at Bodega Butte (Fig. 3A). This suggests that some Canovas Canyon lava domes are only slightly younger than the basalt of Chamisa Mesa.

The small lava dome on the south end of Loma Creston (Fig. 3A) yielded a whole rock age of 9.72± 0.14 Ma, although the age spectrum was somewhat disturbed (Table 1, no. 23). Glassy lava exposures at the north edge of the quadrangle represent the toes of flows contiguous with the Borrego lava dome in the Bear Springs Peak quadrangle (Fig.1; Kempter et al., 2003). The 9.5 Ma age of the Canovas Canyon flow shown in the correlation diagram at Borrego Mesa (Fig. 3A) is projected from the toe of the flow at Borrego Canyon on the basis of this apparent continuity.

A faulted and silicified lava dome about 2 km SE of Loma Canovas (Fig. 1) was originally correlated with the Canovas Canyon Rhyolite (Smith et al. 1970), but Kelley (1977) later correlated it with the Bearhead Rhyolite. As a test of this correlation problem, we present a low precision isochron age of 9.7 Ma (Table 1, no. 24) obtained from biotite in the silicified rhyolite tephra immediately adjacent to the north margin of the lava dome. The silicified dome is unlikely to be correlative with the Bearhead Rhyolite, which has been dated at 6.0 to 7.0 Ma (Justet and Spell, 2001). Distinctly higher concentrations of immobile niobium in the silicified lava and tuff (30-34 ppm Nb; Table 2, P, W), compared to the Bearhead-derived Peralta Tuff (9-17 ppm Nb; Table 2, B, C, D), also support its original correlation with the Canovas Canyon Rhyolite.

The Canovas Canyon Rhyolite erupted from at least three different centers in or near the study area (Fig. 1). Our preferred age of the Canovas Canyon Rhyolite ranges from 9.7 to 9.4 Ma (Table 4). This includes the age of a Canovas Canyon-derived obsidian pebble collected from a volcanic-rich conglomerate at Loma Canovas (Fig. 3B).

Trachydacite flow at Loma Creston

A 50 m-thick flow of light to medium gray, phenocryst-poor to moderately phenocryst-rich, hornblende-plagioclase-biotite trachydacite that locally caps Loma Creston is a typical lithology of

TABLE 4. Nomenclature and preferred ages of eruption for volcanic strata in the Loma Creston quadrangle.

Stratigraphic Unit	Symbol	Preferred Age (Ma)	Comment
basaltic andesite of San Felipe NW	Tbn	2.46± 0.22	Erupted from isolated fissure vent on NW corner of Santa Ana Mesa
pumice bed from Cerrito Yelo	Tcyt	6.29± 0.08	Maximum age of the upper Cochiti Fm.Late pulse of Bearhead Rhyolite eruption
Cochiti Formation	Tc	2.4 to 6.8	Lower part bracketed by Tbn and Tbps
sedimentary and fall deposits of the Peralta Tuff Member of the Bearhead Rhyolite	Tbps	6.81± 0.08; 7.02± 0.12	Two stratigraphically distinct ash-bed horizons within this unit imply at least two major pulses of eruption. Unconformity at base.
Peralta Tuff Member of the Bearhead Rhyolite	Tbp	6.89± 0.14	Top of composite unit. Angular unconformity at base
trachyandesite of Mesita Cocida, upper member of the Paliza Canyon Formation	Tpmc	**7.09± 0.21** (n=3)	Newly named flow unit. Assigned to Paliza Canyon Formation as its youngest member. Angular unconformity at base.
Arroyo Ojito Formation	Tao	7.1 to 9.1	Locally bracketed by Tpmc and Tpbb
Paliza Canyon Formation volcaniclastic sediments	Tpvs	7.1 to 9.1	Locally bracketed by Tpmc and Tpbb. Intertongues with lower Arroyo Ojito Formation
basalt of Bodega Butte, medial member of the Paliza Canyon Formation	Tpbb	**9.14± 0.12** (n=4)	Newly named, moderately widespread flow unit of the Paliza Canyon Formation. Represents a late-stage eruption on southern flank of composite volcano centered near Ruiz Peak.
trachydacite flow at Loma Creston, lower member of the Paliza Canyon Formation	Tpd	9.44± 0.16	Isolated flow unit, highly lenticular member of the Paliza Canyon Formation in Loma Creston quadrangle
Cerro Conejo Formation (upper member)	Tcj	9.9 to 9.1	Bracketed by Tpbb and Tcb
Canovas Canyon Rhyolite	Tcc	9.38± 0.06; 9.54± 0.14; 9.72± 0.14	Multiple lava domes and tuffs erupted between 9.7 to 9.4 Ma
basalt of Chamisa Mesa, basal member of the Paliza Canyon Formation	Tpcm	**9.9± 0.9** (n=2)	Texturally distinct nearly aphyric diabasic basalt. Reinstated informal flow unit; here assigned to the basal Paliza Canyon Formation. Average of imprecise isochron ages

NOTES: Preferred ages are based on highest quality data available from Table 1. Formally named units are capitalized. Mean age of flow unit is shown in bold font; n is number of determinations used to calculate mean. Sedimentary formations bracketed by the dated units are included in list.

the Paliza Canyon Formation (Lavine et al., 1996). The isolated character of this lenticular flow implies a local vent under Loma Creston, or in the down-faulted block immediately to the east of Loma Creston (Chamberlin, et al., 1999; Smith et al., 1970, cross section D-D'). Map data of Chamberlin et al. (1999) show that the basalt of Bodega Butte forms a continuous mesa cap to the west of Loma Creston. However, structure sections indicate the basalt of Bodega Butte and the dacite flow at Loma Creston occupy the same stratigraphic position (Fig. 3A), which makes their relative ages uncertain.

A relatively precise $^{40}Ar/^{39}Ar$ age of 9.44± 0.16 Ma on biotite from the Loma Creston flow (Fig. 3A, no. 21) implies it is older than the laterally adjacent basalt of Bodega Butte. Presumably the olivine basalt flowed southward around a preexisting low hill of dacite lava at Loma Creston, as illustrated in Figure 3A. Hornblende in this flow also yielded an $^{40}Ar/^{39}Ar$ age of 9.23± 0.96 Ma (Fig.3A, no. 20), which is too imprecise to constrain its stratigraphic position. The trachydacite flow at Loma Creston is coeval with the Paliza Canyon Formation (cf. Lavine et al., 1996) and considered here to be a lower to medial member of that formation.

Basalt of Bodega Butte

The basalt of Bodega Butte is a new informal name assigned here to the dark gray, sparsely porphyritic, olivine basalt that caps the mesa at Bodega Butte (Figs.1, 3). In a graben to the west of Bodega Butte, the same 10 m-thick olivine basalt flow overlies eolian and fluvial sandstones of the Cerro Conejo Formation of Connell (1995) and is overlain by volcanic-rich fluvial conglomerates, here tentatively correlated to the Navajo Draw Member of the lower Arroyo Ojito Formation of Connell (1995). We suggest Bodega Butte and the adjacent graben as a type section for this newly named flow unit. The phenocryst mineralogy of this basaltic flow unit appears to vary laterally from olivine basalt at Bodega Butte to olivine basalt with traces of phyric augite at Borrego Mesa and to olivine-augite basalt at Loma Canovas (Fig.1; Table3, L, M, J, respectively). We suggest the northern half of the Loma Creston quadrangle as a type area for the basalt of Bodega Butte. At the southeastern end of Borrego Mesa the basalt of Bodega Butte lies directly on a thick lava flow of the Canovas Canyon Rhyolite and the underlying sedimentary units (Cerro Conejo Formation? and Paliza Canyon Formation volcaniclastic sediments?) must wedge out northward, although it is difficult to be sure since they are generally covered by colluvium (Fig. 3A).

The basalt of Bodega Butte has produced three relatively precise plateau ages of 9.04 ± 0.12 Ma at Bodega Butte, 9.17 ± 0.10 Ma at southeast Borrego Mesa and 9.04± 0.18 Ma at Loma Canovas (Fig. 3). A slightly disturbed spectrum yielded a lower confidence age of 9.25± 0.13 Ma from a propylitically altered sample collected at Arroyo Arenoso. Within analytical error, all four ages are identical. Major and trace element compositions of the unaltered samples are quite similar (Table 2, L, M). We calculate a weighted mean age of 9.14± 0.12 Ma, based on all four plateau ages. This is the most representative and precise cooling age of the basalt of Bodega Butte.

As defined here, the basalt of Bodega Butte (Fig. 3) is laterally continuous with and correlative to the "olivine basalt member of the Paliza Canyon Formation, Tpob" as mapped by Kempter et al. (2003), in the Bear Springs quadrangle, north of Loma Creston. Detailed map patterns of Kempter et al. (2003) indicate that their olivine basalt member (Tpob) locally overlaps the Canovas Canyon Rhyolite and a lower plagioclase-pyroxene basalt member of the Paliza Canyon Formation. The latter yielded an $^{40}Ar/^{39}Ar$ age of 9.54± 0.08 Ma (Kempter et al., 2003). About 7 km north of Loma Creston the basalt of Bodega Butte ("Tpob" of Kempter et al., 2003) appears to fill southwest descending paleovalleys inset into the lower flank of a large andesitic to dacitic composite volcano of the Paliza Canyon Formation that is centered on Ruiz Peak. The estimated angle of descent of these paleovalleys is approximately 7 degrees to the southwest. Upslope projection of these paleovalleys implies that most, or all, of the volcanic pile under Ruiz Peak predates the basalt of Bodega Butte. Thus the estimated "life span" of the Paliza Canyon volcano at Ruiz Peak is about 0.4±0.15 m.y..

The basalt of Bodega Butte is here assigned to the stratigraphic position of a late-stage flank eruption of mafic lava, perhaps from a fissure vent, near the southern base of a composite volcano in the Paliza Canyon Formation, centered on Ruiz Peak. In the Loma Creston quadrangle, the basalt of Bodega Butte appears to occur near the middle of the Paliza Canyon Formation, but with respect to the composite volcano at Ruiz Peak it apparently occurs in the upper part of the formation. About 2 km east of Loma Canovas a propylitically altered outcrop of the basalt of Bodega Butte (Table 2, K) locally overlies silicified bedded tephra of the Canovas Canyon Rhyolite and lies below a silicified trachyandesite porphyry lava flow of the upper Paliza Canyon Formation (Fig. 2; Table 2, I). The sample of trachyandesite porphyry listed in Table 2 is from an unaltered zone at this locality (Table 3, I).

Trachyandesite of Mesita Cocida

A 30 m-thick**,** dark gray, microvesicular, microporphyritic, plagioclase-hornblende trachyandesite flow that caps Mesita Cocida is here informally named the trachyandesite of Mesita Cocida (Figs.1, 2, 3B; Tables 2). The south and southeast flank of Mesita Cocida are suggested as a type section for this mafic flow unit (Fig. 3B). In thin section, this texturally distinct lava contains a seriate continuum of abundant (30%) microphenocrysts of plagioclase (0.1-1.0 mm) and sparse small needles of hornblende (Table 3, F, G, H). Trace amounts of fine-grained olivine, completely replaced by iddingsite, suggest this andesitic lava is of hybrid origin and that it contains a basaltic component. The basal 6 to 9 m of this aphanitic looking flow is usually a platy nonvesicular zone. The blocky upper zone is typically microvesicular and readily fractures with a sonorous "clink" when struck with a hammer blow. In thin section, the small vesicles display a diktytaxitic texture where plagioclase microlites commonly protrude into the center of the jagged vesicles.

Three samples from the trachyandesite Mesita Cocida have produced plateau ages of 7.18± 0.26, 7.16 ± 0.13, and 6.79± 0.24

Ma from outcrops at Mesita Cocida, Loma Canovas and southwest of Loma Canovas, respectively (Figs. 1, 3; Table 1). From these three age determinations we calculated a weighted mean age of 7.09± 0.21 Ma, which is in good agreement with stratigraphic relationships to other dated strata at Mesita Cocida and Loma Canovas (Fig. 3B).

The trachyandesite of Mesita Cocida is continuous with and correlative to the "basaltic andesite member of the Paliza Canyon Formation (Tpba)" as mapped by Kempter et al. (2003) in the Bear Springs Peak quadrangle. Although now faulted and eroded, the overall initial geometry of the trachyandesite of Mesita Cocida appears to be that of a 6 km-long, tongue-like lava flow gently descending from the north end of Loma Canovas toward its terminus at the south end of Mesita Cocida. A vent area is not evident at the north end of Loma Canovas, but a similar looking mafic dike about 2 km south of Bear Spring Peak may represent a potential source (K. Kempter, personal commun., 2005). The base of the essentially horizontal trachyandesite flow at Mesita Cocida is an angular unconformity with an angular divergence of about 7º to the underlying volcaniclastic sedimentary beds. We tentatively assign the trachyandesite of Mesita Cocida to the Paliza Canyon Formation, as its youngest known member (cf. Lavine et al., 1996).

Peralta Tuff and coeval ash beds

The Peralta Tuff is the formally named pyroclastic member of the Bearhead Rhyolite (Bailey et al., 1969). In the study area, the Peralta Tuff consists of light gray to white, glassy to lithoidal, pumiceous bedded tuffs. Intercalated fall deposits, indicated by graded bedding, and pumiceous sandstone beds of fluvial origin comprise most of the unit here. One debris-flow bed is present in the Peralta Tuff exposure southeast of Mesita Cocida (Fig.1, near no. 12). Abundant small cobbles of phenocryst-poor rhyolite and a few small boulders of mafic lava, in a tuffaceous sandy matrix, distinguish it from the surrounding pumiceous beds. Abundant pumice lapilli are rhyolitic (Fig. 2; Table 2) and characterized by sparse, fine- to medium-grained phenocrysts of sanidine, biotite, plagioclase, and traces of quartz.

A sanidine-biotite-plagioclase rhyolite ignimbrite occurs at the top of a zone of silicified bedded tuffs exposed in the ridge crest about 2 km southeast of Mesita Cocida (Fig.1, no. 11). Unaltered clear sanidine from this thin tuff yields a precise single-crystal laser-fusion age of 6.89± 0.14 Ma (Table 1, no. 11), which is our preferred age for the Peralta Tuff in the study area (Table 4). This silicified tuff outcrop was previously miscorrelated with the tephra facies of the Canovas Canyon Rhyolite (Smith et al., 1970). $^{40}Ar/^{39}Ar$ age determinations of 6.76 to 6.96 Ma have been reported for the main pulse of Peralta Tuff eruptions in the Santo Domingo Basin (Smith et al., 2001, table 2, fig. 5d; multiply by 1.0065 for comparison to 28.02 Ma monitor age used here). Distal fall deposits of the Peralta Tuff in the Española basin also fall in this age range (McIntosh and Quade, 1995). Our preferred age for the Peralta Tuff is in good agreement with this published data. Sanidine in rhyolite pumice from the down-faulted block of Peralta Tuff southeast of Mesita Cocida has produced a less precise but analytically equivalent age of 6.73± 0.38 Ma (Fig. 3B).

Thin discontinuous beds of pumiceous ash and pumiceous sandstone coeval with the Peralta Tuff occur within a 50 to 60 m-thick sequence of fluvial tuffaceous sandstones and volcanic-derived conglomerates that are locally inset against the trachyandesite of Mesita Cocida west of Borrego Canyon (Fig. 1, nos. 3-10). This water-laid volcaniclastic sedimentary unit, characterized by numerous pumiceous beds, has been designated as the sedimentary facies of the Peralta Tuff (Table 4; G. Smith, personal commun., 2005). Eight age determinations from the pumiceous beds range from 6.79 to 7.03 Ma (Table 1, nos. 3-10), which demonstrates this sedimentary unit is age equivalent to the main pyroclastic phase of the Peralta Tuff (Smith et al., 2001). The sedimentary facies of the Peralta Tuff unconformably overlies granite-sourced conglomerates and quartzo-feldspathic sandstones of the Loma Barbon member of the Arroyo Ojito Formation in the shallow graben between Loma Creston and Mesita Cocida (Chamberlin et al., 1999). This tuffaceous sedimentary unit grades upwards into the Cochiti Formation, as defined by Smith and Lavine (1996).

A pumiceous sandstone bed within the Cochiti Formation on the south wall of Borrego Canyon (Fig.1, no. 2) yielded a sanidine age of 6.29± 0.08 Ma (Tables 1, 2), which indicates it is temporally equivalent to the youngest pulse of plinian Bearhead Rhyolite eruptions associated with the lava dome at Cerrito Yelo (Smith et al., 2001; Justet and Spell, 2001). It is informally designated here as the pumice bed from Cerrito Yelo (Table 4).

Basaltic andesite of San Felipe–northwest

Basaltic lavas and cinder cones that cap Santa Ana Mesa have been informally referred to as the "basalt of the San Felipe volcanic field" (Smith and Kuhle, 1998). An aeromagnetically defined basaltic flow unit, apparently erupted from an isolated fissure vent on the northwest corner of Santa Ana Mesa, is here referred to informally as the basaltic andesite of San Felipe– northwest (Fig. 1; Table 4). A small lava outcrop west of Borrego Canyon road consists of medium gray, phenocryst-poor, olivine basaltic andesite with traces of fine-grained plagioclase and xenocrystic quartz (Table 3). This lava produced an $^{40}Ar/^{39}Ar$ plateau age of 2.46± 0.22 Ma from a groundmass separate (Table 1, no. 1); chemically it is a low-silica basaltic andesite (Fig. 2). At the dating locality, the flow appears to be about 6 m thick and has been gently tilted to the east. Topographic relief at the dike-like vent suggests as much as 18 m of tephra surrounds the vent. Smith and Kuhle (1998) reported $^{40}Ar/^{39}Ar$ ages of basalts from northeastern Santa Ana Mesa that range from 2.62± 0.15 to 2.41± 0.03 Ma.

PROVENANCE OF VOLCANICLASTIC SEDIMENTARY UNITS

Indurated conglomerate beds in the Paliza Canyon Formation volcaniclastic sediments and the younger volcanic-derived Cochiti Formation (Table 4) commonly contain sparse small pebbles of black obsidian that are partially to almost completely replaced by light gray, flaky perlite. Field observations show that

the ratio of perlite to obsidian noticeably decreases upwards in stratigraphic sections over 30 m in thickness (Chamberlin et al., 1999). Thus the progressive in-situ replacement of obsidian pebbles by perlite, through slow diffusion of meteoric water into the nearly anhydrous glass, can be used in the field as a crude clock to visually estimate the relative stratigraphic position of volcaniclastic sediments from one fault block to the next. Potassium-rich obsidian pebbles are also excellent candidates for $^{40}Ar/^{39}Ar$ age determinations that can help identify their source.

An obsidian pebble, collected from a volcanic-rich conglomerate on the south nose of Loma Canovas, yielded a resistance-furnace plateau age of 9.38± 0.06 Ma (Fig. 1, no. 29; Table 1, no. 29). This is the maximum age for the host Paliza Canyon volcaniclastic sedimentary facies, which is in agreement with the 7.1 Ma age for the overlying trachyandesite flow (Fig. 3B). This obsidian pebble is coeval with and presumably derived from lava domes of the Canovas Canyon Rhyolite near Borrego Canyon (Table 1, no. 22).

An obsidian pebble collected from the Cochiti Formation in lower Borrego Canyon (Fig.1, no. 28; Table 1, no. 28) produced a plateau age of 6.35± 0.20 Ma, thereby indicating that it was derived from erosion of a glassy lava flow equivalent to the Bearhead Rhyolite. In practice, mapping the contact between Paliza Canyon volcaniclastic sediments and younger volcanic-rich Cochiti Formation is nearly impossible, if Peralta ash beds are not present (S.A. Kelley, personal commun. 2006). We suggest that the composition and age of obsidian clasts in volcanic-rich gravels may locally help determine their provenance and correlation, especially where Peralta ash beds are absent.

HYDROTHERMAL ALTERATION AND STRUCTURAL PATTERNS

Zones of hydrothermal silicification are related to Neogene rift faults in the Loma Creston quadrangle (Fig. 4). Narrow ridges of silicified Santa Fe Group sandstone, conglomerate and intercalated volcanic strata locally define silicified footwalls of the rift faults (Figs.1, 5). Minor occurrences of manganese oxides and pyrite within these silicified zones (Fig. 4) confirm that they are of hydrothermal origin.

Field relationships demonstrate that the western belt of light gray chalcedonic alteration is older than the eastern belt of jasperoidal alteration (Fig. 4). Chalcedonic silicification and alteration along the Santa Ana and North Creston fault zones cuts strata as young as the 9.1 Ma basalt of Bodega Butte, but a 6.9 Ma Peralta ash bed immediately adjacent to the north Creston fault is unaltered (Fig.1, no. 8; Table1). In contrast, the younger jasperoidal zone cuts across Peralta Tuff beds in the footwall of the Oso fault, southeast of Mesita Cocida (Figs.1, 4).

The chalcedonic zone lies south of a cluster of Canovas Canyon Rhyolite lava domes (Smith et al., 1970; Kempter et al., 2003), dated here at 9.4–9.7 Ma (Table 1, nos. 22-24). As previously described, the distribution of the basalt of Bodega Butte implies a south-facing paleoslope at 9.1 Ma. We interpret the chalcedonic alteration zone as the product of southerly fault-guided epithermal groundwater flow heated by upper crustal intrusions that

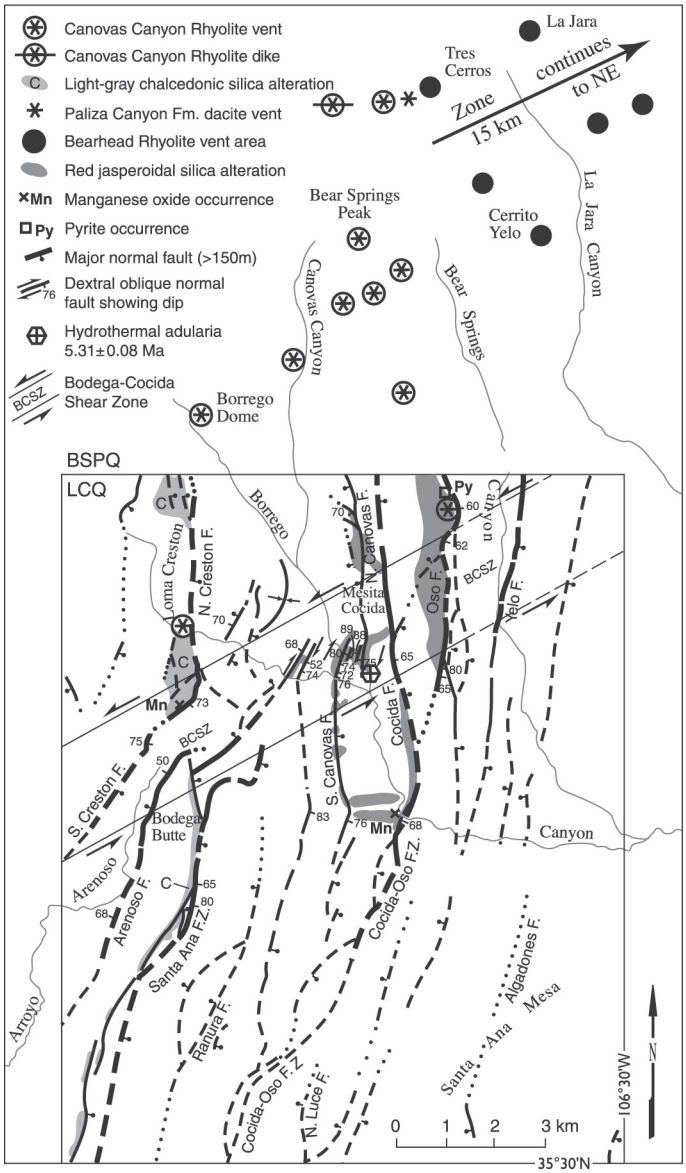

FIGURE 4. Hydrothermal alteration zones and their relationship to normal fault blocks of the Rio Grande rift in the Loma Creston quadrangle (LCQ) and to silicic lava domes of late Miocene age in the Bear Springs Peak quadrangle (BSPQ). Inferred vent locations are from Chamberlin et al. (1999); Smith et al. (1970); and Kempter et al. (2003). Adularia from the red jasperoid zone is dated at 5.31± 0.08 Ma. See text for discussion.

fed the Canovas Canyon Rhyolite. Silicified fault breccias in the Santa Ana zone indicate that some faulting occurred contemporaneous with hydrothermal alteration. Most displacement along the Santa Ana and Creston fault system predates the middle Pliocene Gravel of Lookout Park (Chamberlin et al., 1999). The chalcedonic alteration zone apparently became active after 9.1 Ma and ceased prior to 6.9 Ma.

The younger belt of brick-red jasperoidal silicification occurs along the Cocida, Oso, and Canovas fault zones in the north central sector of the quadrangle (Fig. 4). The jasperoidal belt lies southwest of a 20 km-long, ENE-trending belt of lava domes

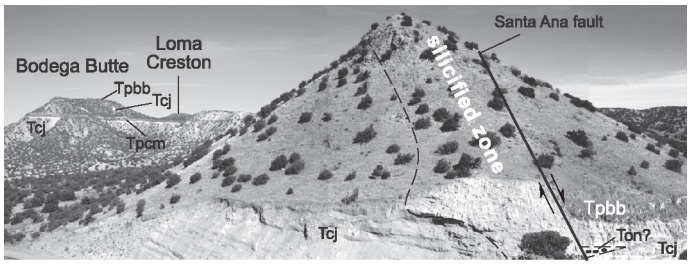

FIGURE 5. 20 m-wide zone of chalcedonic silicification cutting across sandstone beds of the Cerro Conejo Formation (Tcj) in footwall of Santa Ana fault at road cut 2.5 km south of Bodega Butte. The 9.1 Ma basalt of Bodega Butte (Tpbb) in the hanging wall is propylitically altered. A lens of volcanic-derived conglomerate (Ton?), contains mostly andesite, basalt and dacite clasts similar to the Paliza Canyon Formation, but sparse clasts of phenocryst-rich, feldspar-quartz-biotite rhyolite also found here represent a lithology unknown in the Paliza Canyon Formation (Lavine et al., 1996). The conglomerate bed is tentatively correlated with the Navajo Draw Member of the Arroyo Ojito Formation. The southern terminus of the basalt of Chamisa (Tpcm) is exposed 0.9 km north of this road cut.

assigned to the Bearhead Rhyolite (Smith et al., 1970; Justet and Spell, 2001; Fig. 4). Hydrothermal adularia, which replaced plagioclase phenocrysts in an altered dacitic ash bed south of Mesita Cocida, was precisely dated at 5.31± 0.08 Ma (Fig. 3B; Table 1, no. 27). These field relationships and age data support the interpretation of the jasperoidal zone as the product of southerly fault-guided epithermal flow heated by upper crustal intrusions that fed the Bearhead Rhyolite from 7.0 to 6.0 Ma (Justet and Spell, 2001). WoldeGabriel and Goff (1989) used the K-Ar method to date two hydrothermal alteration events in the Cochiti mining district, one at 8.1 Ma and another as young as 5.6 Ma. The two episodes of hydrothermal alteration in the Loma Creston Quadrangle appear to be broadly correlative with events in the Cochiti district.

Bodega-Cocida shear zone

The Bodega-Cocida shear zone (BCSZ) is expressed by a 1.5 km-wide, ENE-trending zone of deflections, splays and terminations within the dominant northerly striking array of Neogene rift faults (Chamberlin, 1999; Fig. 4). A belt of six jasperized en echelon faults, which is well exposed for 2 km to the west of Mesita Cocida, provides key kinematic data on the nature of this transverse zone of distributed lateral shear. Sliplines (striations and "Riedel" shears) are locally well preserved and exposed on silicified faces of the Neogene rift faults (Chamberlin et al., 1999, table 4).

Within this belt of jasperized faults (Fig. 4), NNE-striking, moderate throw (10-60 m), normal faults consistently show dextral oblique slip; striae pitch 28-52°S on east-down faults and 11-63°N on west-down faults. Two subvertical faults at the east end of the belt strike more northerly and show nearly pure dextral slip; striae pitch at 2-8°N. This en echelon belt of dilation and lateral shear is interpreted here as a transverse zone of distributed sinistral shear that was active during jasperoidal alteration about 5.3 m.y. ago. Dextral slip within the en echelon belt at Mesita Cocida is tentatively attributed to counterclockwise "domino-style" rotation of the intervening blocks. Vertical axis rotations cannot be demonstrated at Mesita Cocida but the relationships described above suggest that blocks at the east end of the array are more rotated than those farther west. As discussed below, this interpretation is supported by paleomagnetic studies elsewhere in the Rio Grande rift and the Great Basin. Large displacement normal faults in the study area, such as the Santa Ana, Cocida, and Oso faults dip steeply to the east. They are essentially dip-slip, usually with a minor component of dextral slip (striae pitch 78-87°S).

A paleomagnetic study in the northern Rio Grande rift (Salyards et al., 1994) demonstrated as much as 20° of counterclockwise rotation of Neogene fault blocks adjacent to the ENE-trending Embudo accommodation zone near Española. Hudson et al. (1998) also used paleomagnetic data to delineate a 50 x 120 km long zone of distributed sinistral shear associated with counterclockwise rotation of dextral-slip faults at the northwest margin of the Colorado Plateau in southern Utah. By analogy, we suggest that distributed sinistral transtension within the Rio Grande rift can masquerade in near-surface rocks as zones of distributed right-oblique extension, if accompanied by subtle counterclockwise block rotations.

STRUCTURAL CONTROL OF LATE MIOCENE RHYOLITE INTRUSIONS

A tectonic model of the Rio Grande rift proposed by Chapin and Cather (1994, fig. 1) shows the relatively rigid Colorado

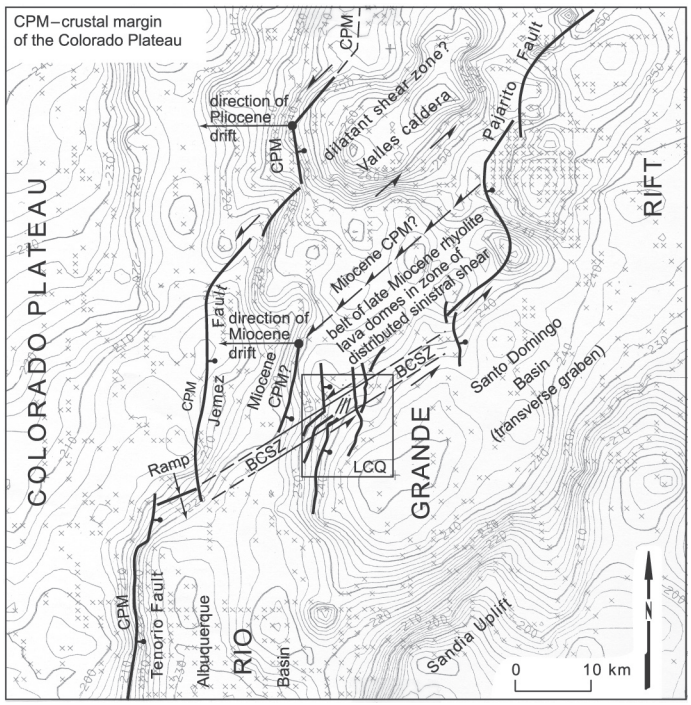

FIGURE 6. Bouguer gravity map of the northern Albuquerque Basin; modified after Keller and Cordell (1983). Thin parallel lines labeled BCSZ indicate the axis of an ENE-trending narrow zone of distributed sinistral shear here termed the Bodega-Cocida shear zone. Rectangle labeled "LCQ" shows outline of the Loma Creston 7.5-minute quadrangle. See text for discussion.

Plateau moving westward away from the axis of the Rio Grande rift. This model predicts zones of concentrated sinistral oblique extension anywhere a "rigid" shoulder of the Colorado Plateau juts eastward against relatively hot and plastic lithosphere under the rift. At the latitude of the Jemez Mountains, rift basins step eastward across the inferred ENE-trending structural grain of the Jemez lineament, which has been embedded within cratonic North America since middle Proterozoic time (Karlstrom and Humphreys, 1998).

Regional patterns suggest that the Bodega-Cocida shear zone (BCSZ) represents deflections and terminations of north and south propagating rift faults by a pre-existing basement shear zone. A regional Bouguer gravity map (Fig. 6) shows that the BCSZ is aligned with a large SE-dipping relay ramp that links the Tenorio and Jemez faults near the west margin of the Albuquerque Basin. The BCSZ is also aligned with a prominent NE-trending segment of the Pajarito fault. Together, the BCSZ and NE-trending Pajarito fault appear to form the northwest margin of the Santo Domingo subbasin. The BCSZ may represent reactivation the ENE-trending middle Proterozoic structural grain of the Yavapai-Mazatzal suture zone (Karlstrom et al., 1999) by the Rio Grande rift.

As a working hypothesis, we suggest that the BCSZ formed as a relatively "rigid" ENE-trending crustal margin of the Colorado Plateau was dragged obliquely westward away from relatively mobile lithosphere under the Rio Grande rift to create a focus of dilatant sinistral shear. This dilatant shear zone then presumably made room for the rise of late Miocene rhyolite intrusions under the southern Jemez volcanic field (Fig. 6). Two lines of evidence support this hypothesis. First, late Miocene rhyolite intrusions that fed the lava domes are only present north of the BCSZ. Second, most rhyolite vent structures (lava dome crests) are aligned to the ENE or to the east (e.g., Tres Cerros, Fig. 4), which is at a high angle to N-trending vent structures commonly seen elsewhere along the axis of the Rio Grande rift (e.g., Albuquerque volcanoes). We suspect that the E-trending silicic intrusions under Tres Cerros may represent the surface expression of a narrow melt accumulation band that formed by dilatant ductile shear in a partially molten middle crust in late Miocene time (cf. Katz et al., 2006). A NNW-trending zone of lava domes south of Bear Springs Peak suggests that the Oso fault, a brittle upper-crustal structure, was also active in late Miocene time. Finally, we speculate that continued westward drift of the Colorado Plateau in Pliocene and Pleistocene time may have focused dilatant ductile shear of sinistral geometry in the middle crust under what is now the Valles caldera (Fig. 6).

CONCLUSIONS AND DISCUSSION

High-precision $^{40}Ar/^{39}Ar$ dating of volcanic strata in the Loma Creston quadrangle of the southern Jemez volcanic field permits the following conclusions.

1) Volcanic activity began with eruption of the aphyric to phenocryst-poor basalt of Chamisa Mesa at about 9.9±0.9 Ma.

2) The initial basalt eruption was followed shortly thereafter by pasty lava dome and plinian eruptions of the Canovas Canyon Rhyolite from 9.7 to 9.4 Ma, which implies that a typical "bimodal" basalt-rhyolite association began the magmatic evolution of the southern Jemez field.

3) The 9.1 Ma olivine-augite basalt of Bodega Butte was a late-stage flank eruption from a 9.5 Ma andesitic to dacitic Paliza Canyon volcano centered at Ruiz Peak. This distinctive olivine-augite lava flowed southward to, and around, a preexisting low hill of dacitic lava erupted at 9.4 Ma near Loma Creston.

4) Volcaniclastic sediments of the Paliza Canyon Formation were faulted, tilted, and eroded prior to eruption of the 7.1 Ma trachyandesite of Mesita Cocida, which represents a narrow tongue of microporphyritic mafic lava that flowed about 6 km southward to its terminus at Mesita Cocida.

5) Shortly after this small-volume mafic eruption, plinian eruptions of the Bearhead Rhyolite from 7.0 to 6.8 Ma deposited pumiceous beds of the Peralta Tuff that also unconformably buried tilted and eroded volcaniclastic sediments plus a granite-sourced fluvial-fan deposit near Loma Creston.

6) A 6.3 Ma plinian eruption from the lava dome at Cerrito Yelo is recorded by a water-laid pumice bed exposed in lower Borrego Canyon.

7) Finally, a small-volume pancake-like flow of xenocrystic basaltic andesite was erupted at 2.4 Ma from an isolated fissure vent on the northwest corner of Santa Ana Mesa. This "final" basaltic event was part of a large outburst of basaltic volcanism along the Jemez lineament in middle to late Pliocene time (cf. Chamberlin, 2007).

Structural observations in and near the Loma Creston quadrangle suggest that the southern flank of the Jemez volcanic field has been a zone of distributed dilational sinistral shear since the onset of rhyolitic volcanism about 9.7 m.y. ago. Tangible evidence of distributed sinistral shear of latest Miocene age is present in an en echelon belt of jasperized dextral-oblique normal faults at Mesita Cocida; intervening fault blocks presumably rotated counterclockwise as they formed. Hydrothermal alteration and silicification at Mesita Cocida is dated at 5.3 Ma. Our working hypothesis suggests that the relatively "rigid" and locally ENE-trending middle crustal margin of the Colorado Plateau has been pulled obliquely away from the mobile middle crust of the Rio Grande rift to create room for intrusion of rhyolite magmas rising along ENE-trending dilatant zones of ductile sinistral shear. These ENE-trending rhyolite intrusions, perhaps the surface expression of melt accumulation bands in the ductile middle crust, apparently fed numerous late Miocene lava domes under the south flank of the Jemez Mountains.

ACKNOWLEDGMENTS

Geologic mapping of the Loma Creston quadrangle was funded by a matching-funds grant from the STATEMAP Program of the U.S. Geological Survey, National Cooperative Geologic Mapping Program, under USGS award number 1434-HQ-97-AG-0781 to the New Mexico Bureau of Geology and Mineral Resources, P.A. Scholle director. The assistance of quadrangle map coauthors G. A. Smith and K. W. Wegmann in collecting rock samples is grate-

fully acknowledged. Special thanks to Lisa Peters and Rich Esser at the New Mexico Geochronology Research Lab for their part in processing samples and generating the $^{40}Ar/^{39}Ar$ data. The Pueblo of Zia graciously permitted access to their tribal lands during this mapping project. Pueblo manager Peter M. Pino was the key liaison officer who made this mapping effort possible. Figures presented here represent the skillful computer drafting work of Tom Kaus; many thanks Tom. We thank Shari Kelley and Fraser Goff for helpful reviews of the manuscript.

REFERENCES

Aldrich, M.J., 1986, Tectonics of the Jemez lineament in the Jemez Mountains and Rio Grande rift: Journal of Geophysical Research, v. 91, p. 1753-1762.

Bailey, R.A., Smith, R.L., and Ross, C.S., 1969, Stratigraphic nomenclature of volcanic rocks in the Jemez Mountains, New Mexico: U.S. Geological Survey, Bulletin 1274-P, 19 p.

Chamberlin, R. M., 1999, Partitioning of dextral slip in an incipient transverse shear zone of Neogene Age, northwestern Albuquerque Basin, Rio Grande rift, New Mexico (abs.): Geological Society of America, Abstracts with Programs, v. 31, no. 7, p. A-113.

Chamberlin, R. M., 2007, Evolution of the Jemez Lineament: Connnecting the volcanic "dots" through late Cenozoic time: New Mexico Geological Society, 58th Field Conference, Guidebook, p. 80-83.

Chamberlin, R.M., McIntosh W.C., and Eggleston T.L., 2004, $^{40}Ar/^{39}Ar$ geochronology and eruptive history of the eastern sector of the Oligocene Socorro caldera, central Rio Grande rift, New Mexico**:** New Mexico Bureau of Geology and Mineral Resources, Bulletin 160, p. 251-279.

Chamberlin, R. M., Pazzaglia, F. J., Wegmann, K. W., and Smith, G. A., 1999 (revised 2007), Preliminary geologic map of the Loma Creston quadrangle, Sandoval County, New Mexico: New Mexico Bureau of Mines and Mineral Resources, Open-file Digital Map Series OF-GM-25, scale 1:24,000.

Chapin, C. E., and Cather, S. M., 1994, Tectonic setting of the axial basins of the northern and central Rio Grande rift: Geological Society of America, Special Paper 291, p. 5-25.

Connell, S.D., 2004, Geology of the Albuquerque basin and tectonic development of the Rio Grande rift in north-central New Mexico, *in* Mack, G.H., and Giles, K.A., eds., The geology of New Mexico, a geologic history: New Mexico Geological Society, Special Publication 11, p. 359-388.

Connell, S.D, 2006, Preliminary geologic map of the Albuquerque–Rio Rancho metropolitan area and vicinity, Bernalillo and Sandoval Counties, New Mexico: New Mexico Bureau of Geology and Mineral Resources, Open-File Report 496A, scale 1:50,000.

Connell, S.D., Koning, D.J., and Cather, S.M., 1999, Revisions to the stratigraphic nomenclature of the Santa Fe Group, northwestern Albuquerque basin, New Mexico: New Mexico Geological Society, 50th Field Conference, Guidebook, p. 337-354.

Gardner, J. N., and Goff, F., 1984, Potassium-Argon dates from the Jemez volcanic field: implications for tectonic activity in the north-central Rio Grande rift: New Mexico Geological Society, 35th Field Conference, Guidebook, p. 75–81.

Gardner, J. N., Goff, F., Garcia, S., and Hagen, R. C., 1986, Stratigraphic relations and lithologic variations in the Jemez volcanic field, New Mexico: Journal of Geophysical Research, v. 91, p. 1763–1778.

Hudson, M. R., Rosenbaum, J.G., Grommé, C.S., Scott, R.B., and Rowley, P.D., 1998, Paleomagnetic evidence for counterclockwise rotation in a broad sinistral shear zone, Basin and Range province, southeastern Nevada and southwestern Utah: Geological Society of America, Special Paper 323, p.149-180.

Justet, L., and Spell, T.L., 2001, Effusive eruptions from a large silicic magma chamber: the Bearhead Rhyolite, Jemez volcanic field, NM: Journal of Volcanology and Geothermal Research, v. 107, p. 241-264.

Karlstrom, K. E., Cather, S. M., Kelly, S. A., Heizler, M. T., Pazzaglia, F. J., and Ray, M., 1999, Sandia Mountains and Rio Grande rift: ancestry of structures and history of deformation: New Mexico Geological Society Guidebook, 50th Field Conference, Guidebook, p. 155-165.

Karlstrom, K.E., and Humphreys, E.D., 1998, Persistent influence of Proterozoic accretionary boundaries in the tectonic evolution of southwestern North America: interaction of cratonic grain and mantle modification events: Rocky Mountain Geology, v.33, p. 161-179.

Katz, R.F., Spiegelman, M., and Holtzman, B., 2006, The dynamics of melt and shear localization in partially molten aggregates: Nature, v. 442, p. 676-679.

Keller, G. R., and Cordell, L., 1983, Bouguer gravity map of New Mexico, National Geophysical Data Center, NOAA, Washington D. C., scale 1:500,000

Kelley, V. C., 1977, Geology of the Albuquerque Basin, New Mexico: New Mexico Bureau of Mines and Mineral Resources, Memoir 33, 60 p.

Kempter, K.A., Osburn, G.R., Kelley, S., Rampey, M., Ferguson, C., and Gardner, J., 2003 (revised 2004), Preliminary geologic map of the Bear Springs Peak 7.5-minute quadrangle, Sandoval County, New Mexico: New Mexico Bureau of Geology and Mineral Resources, Open-file Geologic Map OF-GM 74, scale 1:24,000.

Lavine, A., Smith, G.A., Goff, F., and McIntosh, W.C., 1996, Volcaniclastic rocks of the Keres Group: insights into mid-Miocene volcanism and sedimentation in the southeastern Jemez Mountains: New Mexico Geological Society, 47th Field Conference, Guidebook, p. 211-218.

LeBas, M.J., LeMaitre, R.W., Streckeisen, A., and Zanettin, B., 1986, A chemical classification of volcanic rocks based on total alkali-silica diagram: Journal of Petrology, v. 27, p. 745-750.

Luedke, R. G., and Smith, R. L., 1978, Map showing distribution, composition, and age of late Cenozoic volcanic centers in Arizona and New Mexico: U.S. Geological Survey, Miscellaneous Investigations Map I-1091A, scale 1:1,000,000.

McIntosh, W.C., and Quade, J. 1995, $^{40}Ar/^{39}Ar$ geochronology of tephra layers in the Santa Fe Group, Espanola Basin, New Mexico: New Mexico Geological Society, 46th Field Conference, Guidebook, p. 279-28

McIntosh, W.C., Peters, L., Chamberlin, R.M., Smith, G.A., and Wegmann, K.G., 2007, $^{40}Ar/^{39}Ar$ dating results for the Loma Creston quadrangle, Sandoval County, New Mexico: New Mexico Geochronology Research Laboratory Open-File Report, OF-AR31 <http://geoinfo.nmt.edu/publications/openfile/argon/home.html>

Osburn, G.R., Kelley, S., Rampey, M., Ferguson, C., Frankel, K, and Pazzaglia, F., 2002, Preliminary geologic map of the Ponderosa 7.5-minute quadrangle, Sandoval County, New Mexico: New Mexico Bureau of Geology and Mineral Resources, Open-file Geologic Map, OF-GM 57A.

Renne, P.R., Swisher, C.C., Deino, A.L., Karner, D.B., Owens, T.L., and Depaolo, D.J., 1998, Intercalibration of standards: absolute ages and uncertainties in $^{40}Ar/^{39}Ar$ dating: Chemical Geology, v. 145, p. 117-152.

Salyards, S.L., Ni, J.F., and Aldrich, M.J. Jr., 1994, Variation in paleomagnetic rotations and kinematics of the north-central Rio Grande rift, New Mexico: Geological Society of America, Special Paper 291, p. 59-17.

Samson, S.D., and Alexander, E.C. Jr., 1987, Calibration of the interlaboratory 40Ar/39Ar dating standard MMhb-1: Chemical Geology (Isotope Geoscience Section), v. 66, p. 27.

Smith, G. A., and Kuhle, A., 1998, Geology of Santa Domingo Pueblo SW quadrangle, Sandoval County, New Mexico: New Mexico Bureau of Mines and Mineral Resources, Open-file Digital Map Series, OF-DM 26, scale 1:24,000.

Smith, G. A., and Lavine, A., 1996, What is the Cochiti Formation?: New Mexico Geological Society, 47th Field Conference, Guidebook, p. 219–224.

Smith, G.A., McIntosh, W.C., and Kuhle, A.J., 2001, Sedimentologic and geomorphic evidence for seesaw subsidence of the Santo Domingo accommodation-zone basin, Rio Grande rift, New Mexico: Geological Society of America Bulletin, v. 113, p. 561-564.

Smith, R. L., Bailey, R. A., and Ross, C. S., 1970, Geologic map of the Jemez Mountains, New Mexico: U.S. Geological Survey, Miscellaneous Geologic Investigations Map I-571, scale 1:125,000.

Steiger, R.H., and Jaeger, E., 1977, Subcommission of geochronology: convention on the use of decay constants in geo- and cosmochronology: Earth and Planetary Science Letters, v. 36, p. 359-362.

WoldeGabriel, G., and Goff. F., 1989, Temporal relations of volcanism and hydrothermal systems in two areas of the Jemez volcanic field, New Mexico: Geology, v. 17, p. 986-989.